Detection of volatile organic compounds using electrospun P3HT/PMMA fibrous film

Ming-Chung Wu [a,b,c,1,*], Shun-Hsiang Chan [a,1], Tz-Feng Lin [a,b], Chun-Fu Lu [d], Wei-Fang Su [d,*]

[a] Department of Chemical and Materials Engineering, Chang Gung University, Taoyuan 33302, Taiwan
[b] Green Technology Research Center, Chang Gung University, Taoyuan 33302, Taiwan
[c] Division of Neonatology, Department of Pediatrics, Chang Gung Memorial Hospital, Taoyuan 33302, Taiwan
[d] Department of Materials Science and Engineering, National Taiwan University, Taipei 10617, Taiwan

ARTICLE INFO

ABSTRACT

Volatile organic compounds (VOCs) sensors are the imperative technology of modern life for environmental monitoring to detect any harmful elements and to prevent lethal exposure. The sensing material is a fibrous film consisting of poly(3-hexylthiophene)(P3HT)/poly(methyl methacrylate)(PMMA) blend, and it is fabricated on a glass substrate. The P3HT/PMMA fibrous film is made by electrospinning process and shows high specific surface for solvent vapor harvesting. The P3HT/PMMA fibrous films are thus easily designed according to the extinction changes of VOCs. The P3HT/PMMA fibrous film exhibits the detection capability for VOCs. It satisfies the detection limit of acetone, toluene and *o*-xylene at 500 ppm. The cost of the P3HT/PMMA fibrous film is acceptable to the market in contrast to the commercial sensors toward VOCs.

© 2017 Taiwan Institute of Chemical Engineers. Published by Elsevier B.V. All rights reserved.

1. Introduction

Volatile organic compounds (VOCs) are hazardous materials to environment and human health. Especially, serious injury and death would occur in the fire and explosion when the concentration of VOCs is above the explosion limit. Thus, the storage, transportation, and usage of VOCs should be very careful to prevent any accident. Further, the sensor needs for VOC is urgent to guard our homeland and defend accidental factors. The sensor design should be real-time detection, high sensitivity and high reproducibility [1–7]. Various sensing materials have been used to detect targeted VOCs, such as conjugating polymers [8], metal oxide [9] and organic/inorganic composites [10].

The physical structure of sensing materials is important to determine the sensitivity of VOCs sensors. The nanostructured sensing materials have been adopted to achieve high sensitivity due to their high surface area [11–14]. Electrospinning technique can be used to prepare a large quantity of sub-microscale or nanoscale diameter of fibrous materials [15,16]. The precursor solution is subjected to a high voltage during the electrospinning process. When the electric field reaches a critical value at which the re-pulsive electric force overcomes the surface tension of solution, a charged jet of the solution is ejected from the tip of the Taylor cone and spun into air as fibers [17,18]. In addition, the electrospinning technique is a simple and economical process to prepare high-performance sensing materials [19,20].

Poly(3-hexylthiophene) (P3HT)/phenyl-C61-butyric acid methyl ester (PCBM) nanocomposites were often used to prepare polymer-based bulkheterojunction photovoltaics [21–24]. In the previous study, a P3HT/PCBM nanocomposite was fabricated as VOCs sensing materials to detect the VOCs existence within several minutes [25]. However, the cost of PCBM is expensive to the industrial production. The electrospun 3D-materials exhibit the larger specific surface area comparing with thin film materials [26]. Electrospinning is a good technique for enhancement of sensitivity and detection limit. Herein, poly(methyl methacrylate) (PMMA) is applied to prepare sensing materials due to the transparent thermoplastic polymer which usually used in sheet form as a lightweight alternative to glass [27,28]. Hence, we adopted the P3HT/PMMA blending system as the sensing material for VOCs detection.

In the present work, we developed a series of P3HT/PMMA fibrous films with various blending ratios by the electrospinning process. The electrospun P3HT/PMMA fibrous film with large specific surface area is a good candidate for VOCs detection. The optical extinction of P3HT/PMMA fibrous film is varied upon the exposure to VOCs vapor, and it served as an indication of the VOCs presence. Furthermore, fast and efficient VOCs sensing is
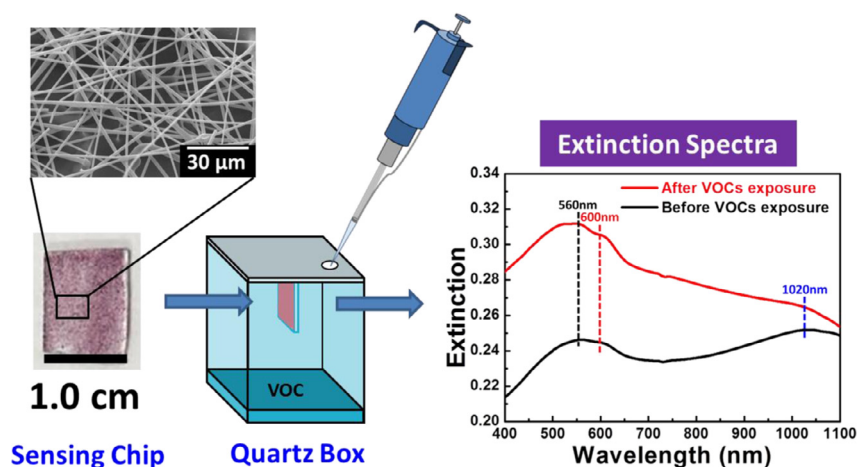
Fig. 1. Illustration diagram of measuring the extinction spectra of the P3HT/PMMA fibrous film before and after 2 h exposure to saturated chlorobenzene.

achievable on the basis of the instant response to the concentration of explosive limit. To the best of our knowledge, this is the first study using P3HT/PMMA fibrous film to detect VOCs [29,30]. The P3HT/PMMA fibrous film developed definitely extends the current VOCs sensing technology and protects human and environment effectively in prior to potential VOCs risks.

2. Experimental details

2.1. Materials

PMMA (M.W. $\sim$ 996,000 Da, Aldrich) was used as received without any purification. The P3HT (M.W. $\sim$ 60,000 Da) was synthesized according to the literature [31]. The P3HT solution was obtained by dissolving P3HT in chlorobenzene (99.8%, Acros) with continuous stirring at 40 °C for 48 h. Then, the P3HT solution was added to the stirred solution of PMMA in chlorobenzene. The details of the chemical composition of the polymer blendings were summarized in Table S1. The concentration of P3HT/PMMA blending solution was 15.0 wt%.

2.2. Fabrication of P3HT/PMMA fibrous film

The electrospinning system includes the high-voltage power supply (You-Shang Technical Co. Ltd., Taiwan), the syringe pump (KDS-100, KD Scientific Inc., United States), and a grounded aluminum disk as the collector (the diameter is $\sim$20.0 cm). The high-voltage power supply gives the maximum voltage of 40.0 kV with the controlled 1.0 V resolution. The syringe pump has the capacity to handle various syringes with different volume and needle size. It precisely controls the flow rates and volumes. The rotational speed of the aluminum disk collector can be tuned precisely. The P3HT/PMMA fibrous films were prepared on the glass substrates successfully regarding the well-defined processing parameters of electrospinning. Generally, the applied voltage is 5.0–25.0 kV; the tip-to-collector distance is 5.0–15.0 cm; the rotational speed of the aluminum disk collector is 50–100 rpm; and the flow rate of P3HT/PMMA blending solution is 0.5–1.5 ml/h. The best conditions in this study are set at 15.0 kV for the applied high-voltage, the tip-to-collector distance at 7.0 cm, the rotational speed of the aluminum disk collector at 80 rpm, and the constant flow rate at 1.0 ml/h. In addition, we also adopted a spin-coater to fabricate a P3HT/PMMA thin film ($\sim$800 nm). The spinning receipt is 500 rpm for 30 s.
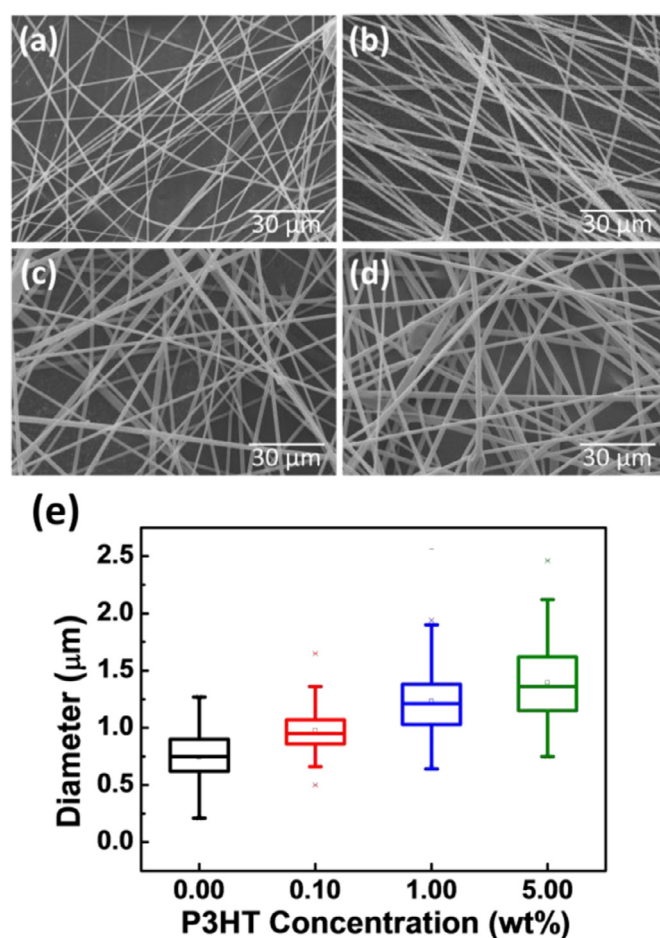

Fig. 2. The SEM images of P3HT/PMMA fibrous film with several P3HT concentrations, (a) pristine PMMA, (b) 0.10 wt% P3HT, (c) 1.00 wt% P3HT, (d) 5.00 wt% P3HT and (e) the diameter distribution of P3HT/PMMA blend fibers.

2.3. Characterizations

The microstructures of P3HT/PMMA fibrous films were observed by scanning electron microscope (SEM, SNE-4500M, SEC Co. Ltd., Korea) that was operated at an accelerating voltage of 15.0 kV. The morphology changes of P3HT/PMMA fibrous film after the treatment of saturated toluene was evaluated by an optical microscope (OM, H416-T, Hwatang Optical Industries Co. Ltd.,
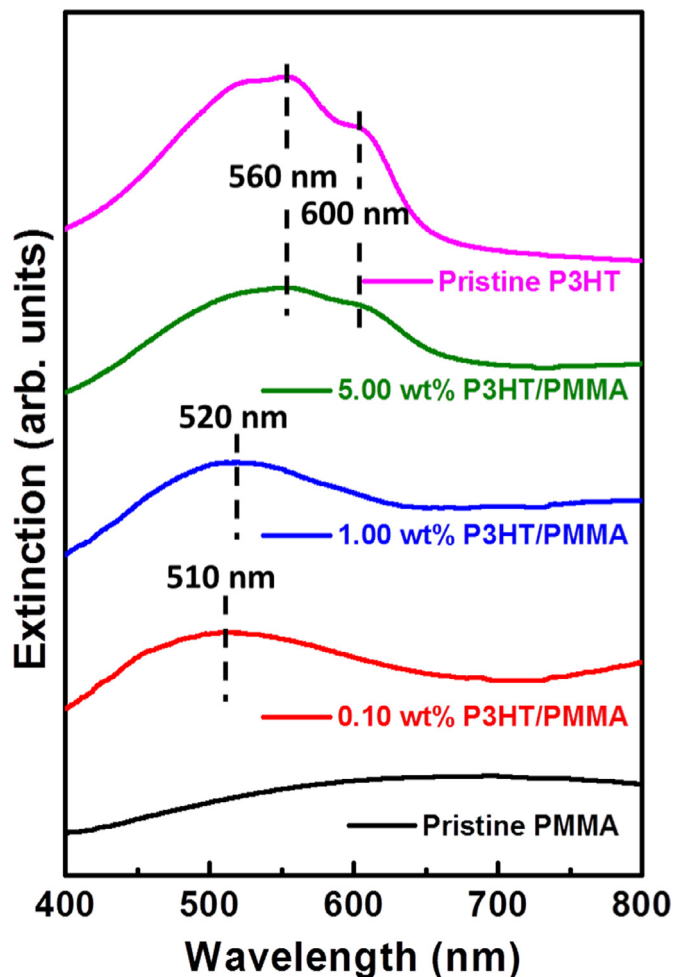
Fig. 3. Plots of extinction spectra of pristine PMMA thin film, 0.10 wt%, 1.00 wt%, 5.00 wt% P3HT/PMMA fibrous films, and pristine P3HT thin film (bottom to the top).

Fig. 4. (a) Photoluminescence spectra and (b) time-resolved photoluminescence spectra of pristine P3HT thin film and various P3HT/PMMA fibrous films with several P3HT concentrations at room temperature.

Taiwan). The steady-state photoluminescence (PL) spectra were obtained by pumping the samples with a continuous wave, diode laser ($\lambda_{exe} \sim 440$ nm, PDLH-440-25, DongWoo Optron Co. Ltd., Korea). The emission spectra were detected by a photomultiplier tube detector system (PDS-1, DongWoo Optron Co. Ltd., Korea) and analyzed by a monochromator (Monora 150i, DongWoo Optron Co. Ltd., Korea). Time-resolved photoluminescence (TRPL) spectroscopy was performed by using a time-correlated single photon counting (WELLS-001 FX, DongWoo Optron Co. Ltd., Korea) spectrometer. A pulse laser ($\lambda_{exe} \sim 440$ nm) with an average power of 1 mW, operating at 50 MHz, with 70 ps duration was applied for excitation.

2.4. Procedures for the VOCs testing

The extinction spectra of the P3HT/PMMA fibrous film were measured using an ultraviolet–visible spectrometer (UV-VIS Spectrophotometer, V-630, Jasco International Co., Japan) in the wavelength range of 400–1100 nm. The 80.0 cm^3 quartz chamber was constructed to simulate the pollution of VOC environment. Typical solvents, including ethanol (99.5%, Acros), acetone (99.8%, Acros), toluene (99.8%, Acros), o-xylene (97%, Aldrich) and chlorobenzene (99.8%, Acros) were tested to access the sensing properties of P3HT/PMMA fibrous film. To identify the VOC absorbed in the P3HT/PMMA fibrous film quantitatively, the different solvent amounts were placed in the bottom for evaporation. (i.e., certain concentration VOCs). Table S2 lists the solvent amounts for VOC testing in quartz chamber. In addition, a gas
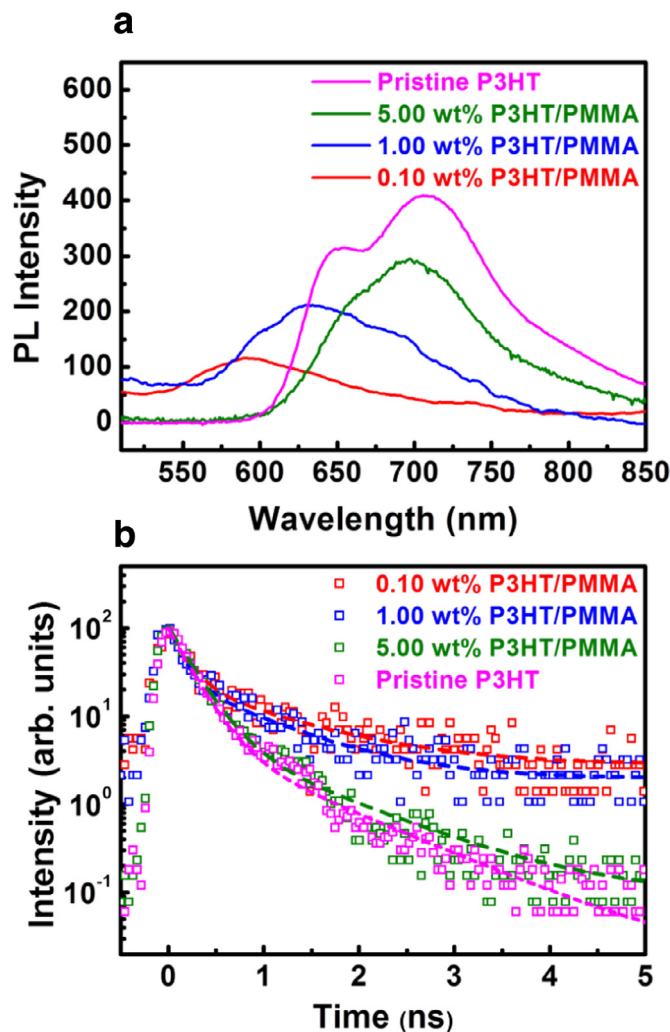
chromatography (GC, 2000, China Chromatography Co., Taiwan) was used to measure the practical VOC concentration again. Each calibration curve is obtained to determine the VOC concentration at first. The theoretical and practical values of VOC concentration are listed in Table S3. For creating saturated VOC vapor pressure, excess solvent was left in the quartz chamber. Whenever solvent is fully evaporated, the P3HT/PMMA fibrous film was placed in the center of the quartz chamber for validation. After that, the ultraviolet-visible spectrometer was utilized to measure the extinction spectrum of P3HT/PMMA fibrous film with VOCs exposed time. The simple illustration diagram of measuring the extinction spectra of the P3HT/PMMA fibrous film is shown in Fig. 1. For the reversibility test of P3HT/PMMA fibrous film, each sample is exposed to the toluene with different concentrations, including 500, 2000, and 10,000 ppm, for 120 min. Then, the chamber was opened and continued to measure the response plots of toluene for 50 min.

3. Results and discussion

Several P3HT/PMMA blend solutions with several P3HT concentrations were prepared to fabricate P3HT/PMMA fibrous films by electrospinning process. The SEM images of various P3HT/PMMA fibrous films are shown in Fig. 2(a)–(d). Fig. 2(e) shows the diameter distribution of various electrospun P3HT/PMMA fibrous films.
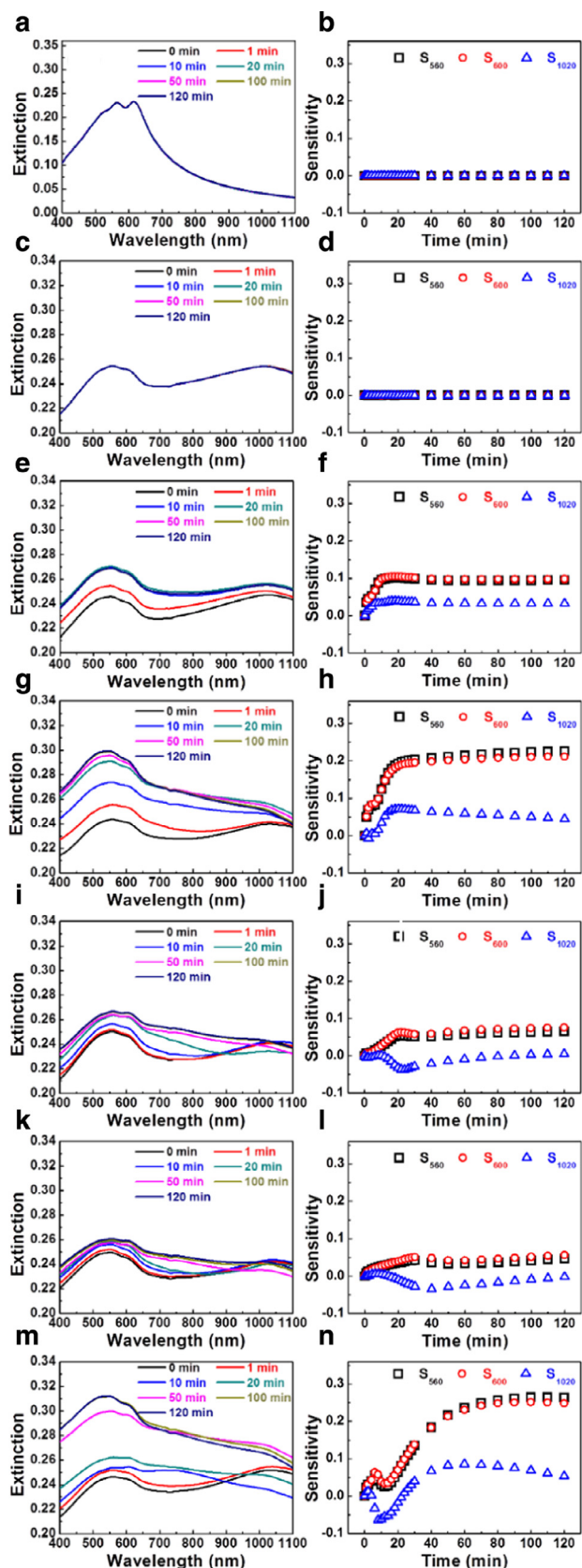
Fig. 5. Extinction spectra and sensitivity plots of P3HT/PMMA blending materials exposed to various VOCs at saturated vapor pressure with different time. (a,b) Blank test for P3HT/PMMA thin film, (c,d) blank test for P3HT/PMMA fibrous film, and P3HT/PMMA fibrous film exposed to (e,f) ethanol, (g,h) acetone, (i,j) toluene, (k,l) o-xylene and (m,n) chlorobenzene.
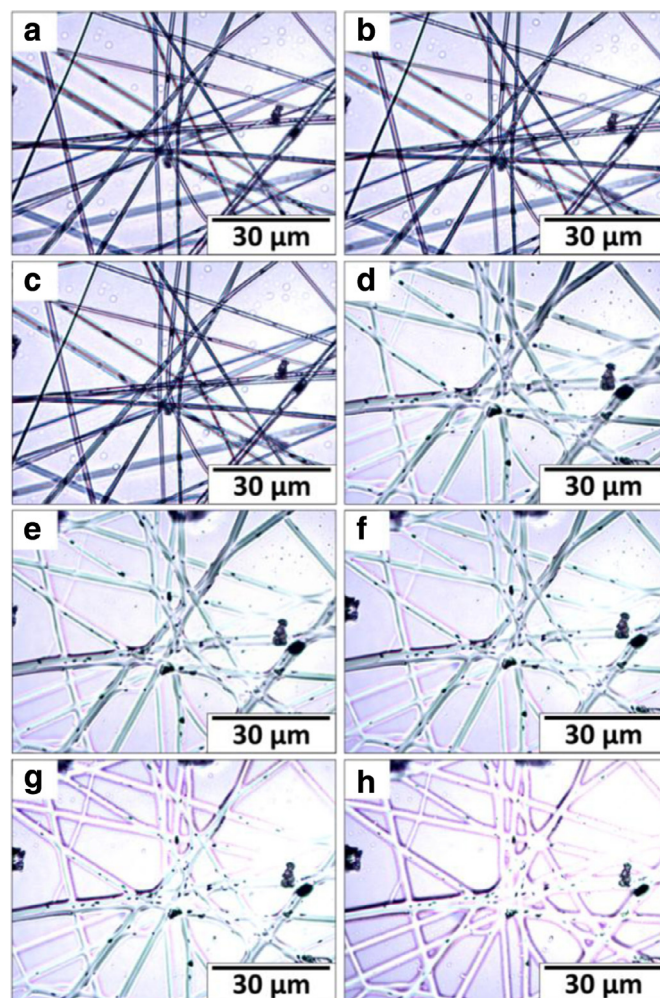
Fig. 6. Optical micrographs of P3HT/PMMA fibrous film exposed to saturated toluene for (a) 0 min, (b) 1 min, (c) 5 min, (d) 10 min, (e) 30 min, (f) 60 min, (g) 90 min and (h) 120 min.
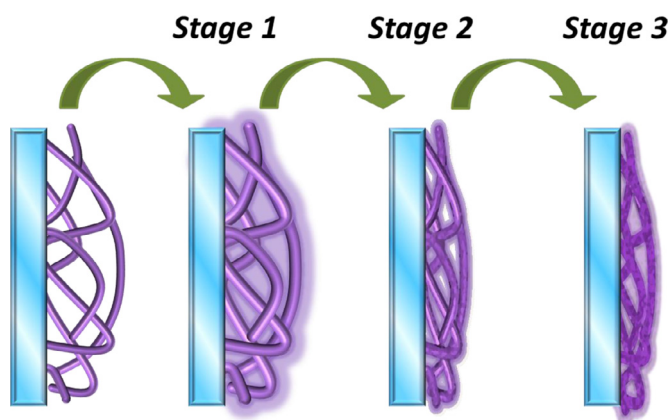
Fig. 7. The schematic diagram of the three stages involved in VOC sensing.

The average diameter is increased from 0.75 μm to 1.40 μm as the concentration of P3HT is varied from 0.00 to 5.00 wt%. It is interesting to know that the thick diameter of 5.00 wt% P3HT/PMMA fibrous film is a result of P3HT–PMMA phase separation [32]. The changes of miscibility of two polymers system are according to the free energy of mixing, which depends on both enthalpy and entropy contributions of each component. For most binary polymeric blends, the entropy of mixing is small, leaving the enthalpy

Table 1
Average lifetime of pristine P3HT thin film and various P3HT/PMMA fibrous films.

P3HT concentration (wt%)	A_1	A_2	τ_1(ns)	τ_2(ns)	Average lifetime (ns)
Pristine P3HT	92.8	6.2	0.21	0.95	0.38
5.00	97.8	6.9	0.23	0.99	0.41
1.00	77.2	25.1	0.13	0.84	0.61
0.10	79.1	22.4	0.16	1.03	0.72

factor to be the determinant [33,34]. Unfavorable enthalpy interaction in polymer blend leads to the extent of phase separation of the blends. Hence, the P3HT-rich domain formation is enhanced in diameter for high P3HT concentration in P3HT/PMMA blends.

Fig. 3 shows the extinction spectra of pristine P3HT, pristine PMMA, and P3HT/PMMA fibrous films with different P3HT concentrations, such as 0.10, 1.00, and 5.00 wt%. The pristine P3HT thin film showed the λ_{max} of extinction spectrum at 560 nm and pronounced 0–0 and 0–1 vibronic band at 600 nm [35,36]. For the extinction spectra of the P3HT/PMMA fibers, it showed a red shift from 510 to 560 nm according to the increment of P3HT concentration. Although the higher P3HT concentration of the P3HT/PMMA fibers could enhance the absorption behavior, the large diameter of fiber could cause the decreased sensing area. In addition, the bead fiber was observed in 10.00 wt% P3HT/PMMA fibrous films due to the lower viscosity and phase separation (Fig. S1). Hence, we proposed that 5.00 wt% P3HT in the P3HT/PMMA blending solution is an optimized condition for sensor application. It has the two characteristic bands at 560 and 600 nm for detecting the absorbance of VOCs.

Fig. 4(a) shows the PL spectra of pristine P3HT thin film and P3HT/PMMA fibrous films with several P3HT concentrations. The maximum peak of PL spectra shows a red shift from 590 nm to 700 nm in the increment of P3HT addition. The PL signal near 700 nm comes from the P3HT-rich domain, and the results are consistent with the trend of extinction spectra as shown in Fig. 3. The TRPL via the time-correlated single photon counting is suitable to measure the fast charge carrier dynamics of P3HT/PMMA fibrous film. The fitting TRPL decay curves at 700 nm for these P3HT/PMMA fibrous films and P3HT thin film are shown in Fig. 4(b). The TRPL spectra are analyzed by bi-exponential decay kinetics after eliminating the instrument response function. The obtained data can be expressed by the Eq. (1) [37,38].

$$F(t) = A_1 \exp\left(-\frac{t}{\tau_1}\right) + A_2 \exp\left(-\frac{t}{\tau_2}\right) \qquad (1)$$

The average lifetime was calculated using the following Eq. (2).

$$t = \sum A_i \tau_i^2 / \sum A_i \tau_i \qquad (2)$$

The average PL lifetimes of the P3HT thin film and P3HT/PMMA fibrous films are shown in Table 1. The PL lifetime of the P3HT/PMMA fibrous film is decreased from 0.72 ns to 0.41 ns with increasing P3HT concentration from 0.10 wt% to 5.00 wt%. The results are expected as the domain size of P3HT is increased. The pristine P3HT thin film shows the similar PL lifetime of 0.38 ns that is consistent to the literature [32]. The electrons generated from P3HT domain is confined in the PMMA matrix which exhibits higher PL intensity and longer lifetime with higher concentration of PMMA.

At first we defined the sensitivity, S_x, of the P3HT/PMMA fibrous film according to the intensity of extinction spectra variation at different wavelength, e.g. 560 nm, 600 nm and 1020 nm, where the suffix x presents the selected wavelength. The S_x equations of the P3HT/PMMA fibrous films are shown at below,

$$S_{560} = \frac{E_{t(560)} - E_{0(560)}}{E_{0(560)}} \qquad (3)$$

$$S_{600} = \frac{E_{t(600)} - E_{0(600)}}{E_{0(600)}} \qquad (4)$$

$$S_{1020} = \frac{E_{t(1020)} - E_{0(1020)}}{E_{0(1020)}} \qquad (5)$$

where $E_{o(x)}$ is extinction signal without VOCs exposure (i.e., 0 min), $E_{t(x)}$ is an extinction signal that is recorded with VOCs exposed time.

The extinction spectra of spin-coated thin film and fibrous film from 5.00 wt% P3HT in the P3HT/PMMA blending solution is shown in Fig. 5(a) and (c). We adopted ethanol, acetone, toluene, o-xylene and chlorobenzene as representing VOCs to test the sensitivity, respectively. The P3HT/PMMA fibrous film was inserted into an 80.0 cm³ quartz chamber to experience the simulated VOCs environment for 2 h. The results are shown in Fig. 5(e, g, i, k and m). Before the fibrous film is exposed to the VOCs, the baseline of the spectra is not horizontally aligned because the P3HT/PMMA fibrous film is not a continuous film. The band at 1020 nm is observed in the fibrous film sample when 3D fibrous structure causes the scattering light. The two bands at 560 nm and 600 nm are from the chromophore and molecular arrangement (crystallinity) of P3HT respectively [36]. Upon VOCs exposure in the quartz chamber, the VOC softens or swells the fibers that fill air voids in the fibrous structure. The spectra baseline moves upward and becomes horizontally aligned, and the 1020 nm band disappears. The extent of changes depends on the behavior of fibrous swelling. For ethanol (Fig. 5(e)), the baseline is a little upward and the 1020 nm band is reduced due to the fulfilled air voids of 3D fibrous structure. Similarly, the band of 1020 nm is disappeared for acetone (Fig. 5(g)) even PMMA is selectively dissolved and the baseline is upward a lot. Similar phenomena are observed for toluene (Fig. 5(i)), o-xylene (Fig. 5(k)) and chlorobenzene (Fig. 5(m)), those VOCs are good solvent for P3HT/PMMA blends, and the band of 1020 nm deteriorates sharply. These features are thus identified as the indication of VOC sensing. The plots of sensitivity versus time of P3HT/PMMA fibrous film exposed to various saturated VOCs are shown in Fig. 5(b, d, f, h, j, l and n). For the blank tests, P3HT/PMMA thin film (Fig. 5(b)) and 5.00 wt% P3HT in the P3HT/PMMA fibrous film (Fig. 5(d)) shows no noticeable changes. In Fig. 5(f, h, j and l), the S_{560} and S_{600} exhibit the same trend for exposure in ethanol, acetone, toluene and o-xylene due to the VOCs adsorption behavior on P3HT/PMMA sensing material. The S_{1020} of ethanol (Fig. 5(f)) shows the equilibrium over 5 min. The S_{1020} of acetone (Fig. 5(h)) exhibits small decreasing over 20 min due to the change of fibrous structure. For exposure to toluene (Fig. 5(j)) and o-xylene (Fig. 5(l)), the S_{1020} gives the same results. Especially, the S_{1020} of chlorobenzene (Fig. 5(n)) reveals complicated variation. For the S_{1020}, the variation is attributed to the morphology change of 3-dimensional P3HT/PMMA fibers, which is confirmed by optical microscope study and discussed below (Fig. 6).

Toluene is extensively used as an industrial feedstock and solvent. It was selected to observe the morphology changes of three-dimensional fibrous film. There is no appearance difference of P3HT/PMMA fibers that are exposed to saturated vapor pressure of toluene less than 5 min (Fig. 6(a)–(c)). The line of S_{1020} plot only shows a minor upturn (Fig. 5(j)). The minor change in sensitivity
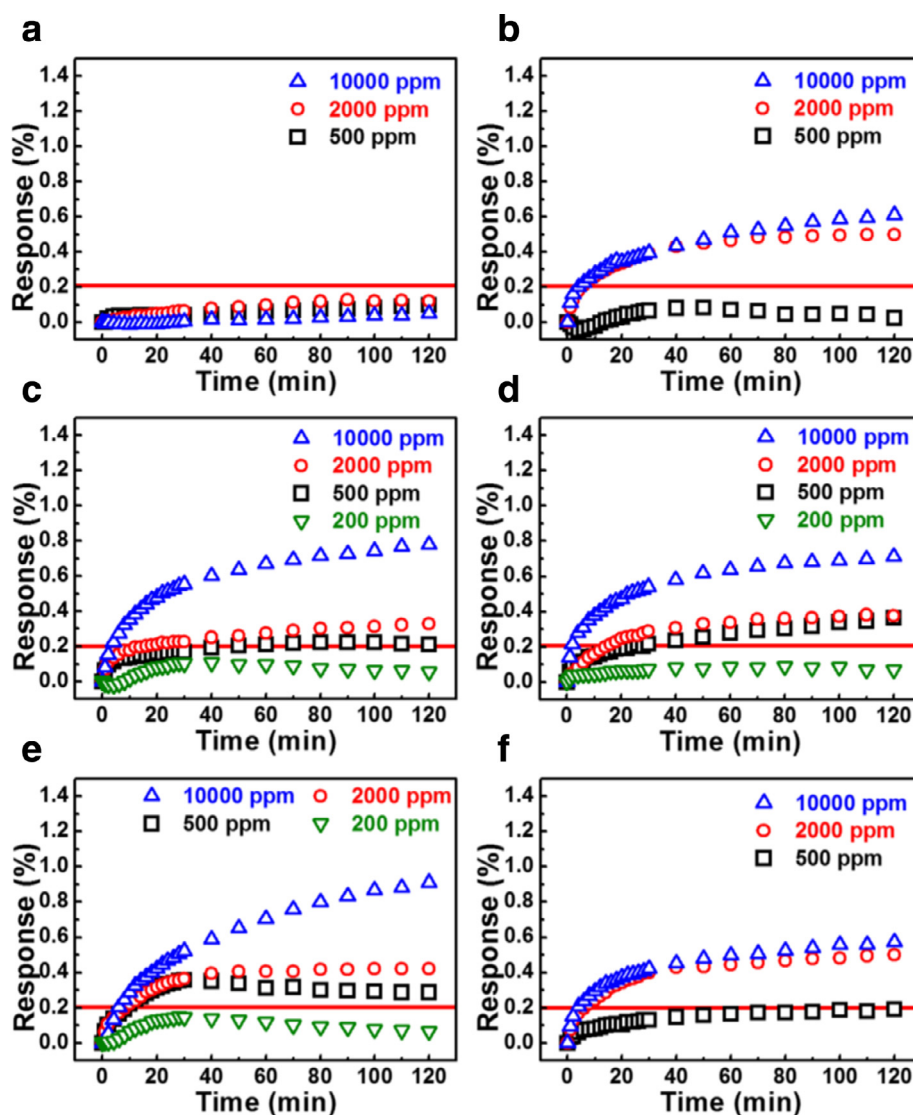
Fig. 8. Response plots at 600 nm for P3HT/PMMA fibrous films exposed to different VOCs concentrations through time, including (a) water, (b) ethanol, (c) acetone, (d) toluene, (e) *o*-xylene and (f) chlorobenzene.

is due to the toluene adsorption and swelling behavior that increased the total volume of P3HT/PMMA. The three-dimensional P3HT/PMMA fibers started to collapse and form flat ribbons and belts due to VOCs vapor exposure (*i.e.*, extended absorption and swelling) over 10 min (Fig. 6(d)). Moreover, the line of S_{1020} plot shows a decline as shown in Fig. 5(j). The P3HT/PMMA flat ribbons and belts are totally swelled when saturated toluene vapor is exposed over 20 min (Fig. 6(e)–(h)). The line of S_{1020} plot is flatted out (Fig. 5(j)). We speculate that there are three stages involved in VOC sensing as illustrated in Fig. 7. At the first stage, VOC was adsorbed on the surface of three-dimensional P3HT/PMMA fibrous film. At the second stage, the three-dimensional P3HT/PMMA fibrous film started to collapse due to polymer relaxation/swelling in VOC vapor. In the last stage, the collapsed P3HT/PMMA fibrous structure was continuously adsorbed and swelled by VOC, the scattering effect of three-dimensional structure was disappeared.

For low concentration VOCs sensing, the band intensity at wavelength of 560 nm and 600 nm is an indicator. The reason is the extinction band at the wavelength of 1020 nm only varied when P3HT/PMMA fibrous film was exposed to the high concentration of VOCs. Various concentrations of toluene (200–10,000 ppm) were evaluated. The response (R_{560} and R_{600}) are defined as below,

$$R_{560} = \frac{E_{t(560)} - E_{0(560)}}{E_{0(560)}} * 100\% \tag{6}$$

$$R_{600} = \frac{E_{t(600)} - E_{0(600)}}{E_{0(600)}} * 100\%. \tag{7}$$

Plots of R_{560} and R_{600} *versus* time are shown in Fig. S2 and Fig. 8, respectively. The response R_{560} and R_{600} of P3HT/PMMA fibrous film is significant as the increased VOC concentration. We define the response time of the fibrous film so that it meets certain concentration of VOC at the response level of larger than two times of the sensing error (~0.20%) at specific wavelength of spectrum. The response time of the P3HT/PMMA fibrous film exposed to particular VOCs were evaluated and the results were summarized in Table 2. The response time measured at the wavelength of 600 nm is usually shorter than the response time measured at the wavelength of 560 nm due to the change of crystallinity of P3HT is larger than the change of chromophore structure when the film is exposed to VOCs. The response time is less than 6 min when the VOCs are at 10,000 ppm regardless their type. The detection limit for ethanol and chlorobenzene is about 2000 ppm, but for acetone, toluene and *o*-xylene is about 500 ppm.
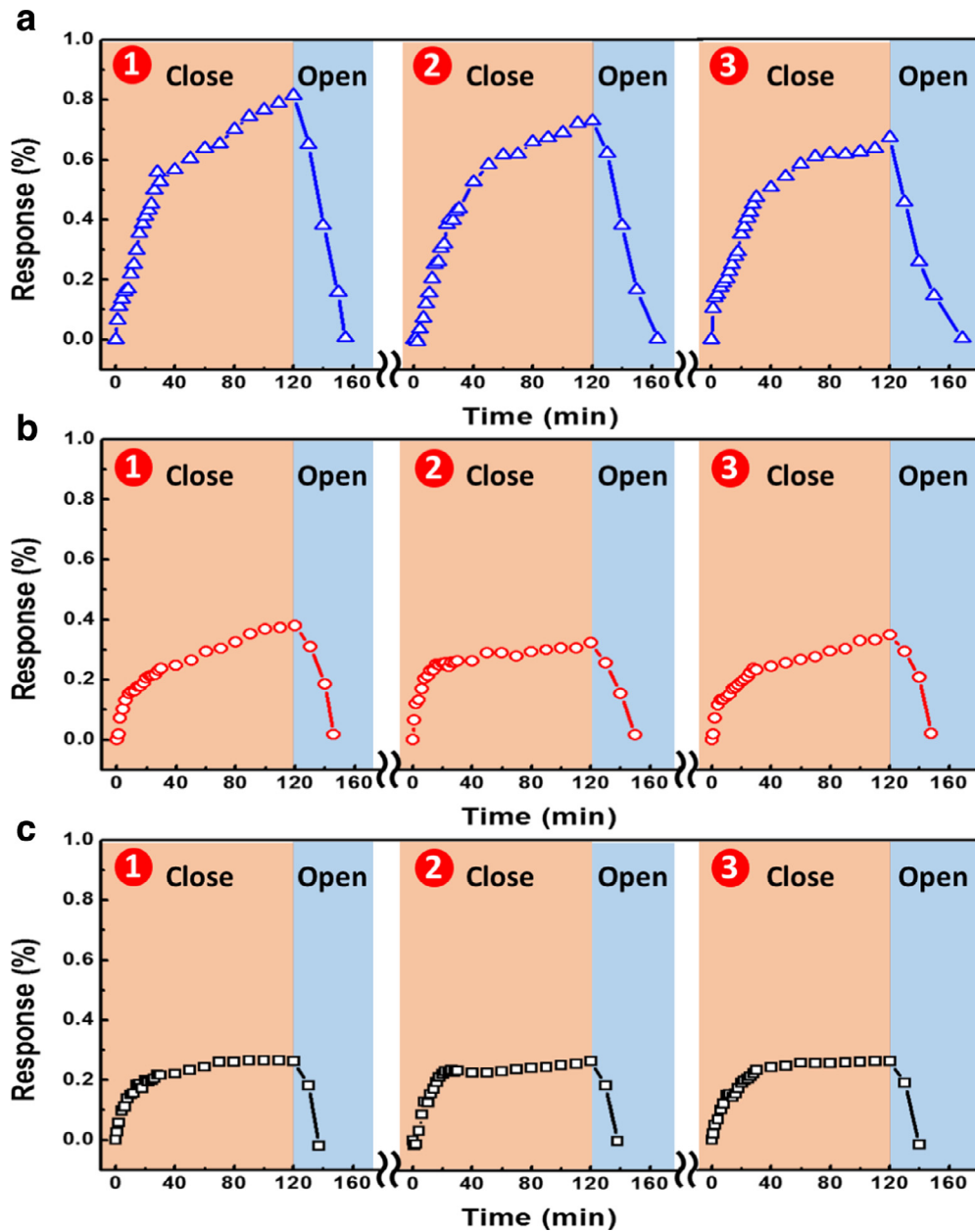
Fig. 9. Reversibility tests of P3HT/PMMA fibrous film exposed to different toluene concentration, including (a) 10,000 ppm, (b) 2000 ppm, and (c) 500 ppm. Each sample is exposed to the toluene with different concentration for 120 min at first.

Table 2
List of response time for P3HT/PMMA fibrous film exposed to various VOCs with different concentrations [25,38].

Type of VOCs	Lower explosive limit (ppm)	Detecting wavelength (nm)	Response time (min) at concentration (ppm)			
			10,000	2000	500	200
Water	..	560	N/A	N/A	N/A	N/A
		600	N/A	N/A	N/A	N/A
Ethanol	33,000	560	4	6	N/A	N/A
		600	4	6	N/A	N/A
Acetone	26,000	560	4	18	50	N/A
		600	4	16	50	N/A
Toluene	12,000	560	2	18	24	N/A
		600	2	16	24	N/A
o-Xylene	10,000	560	6	10	10	N/A
		600	6	10	10	N/A
Chlorobenzene	18,000	560	6	8	N/A	N/A
		600	4	8	N/A	N/A

Actually, the response time for 10,000 ppm toluene is only 2 min. As expected, the response time is longer for low concentration of VOCs. For instance, the response time is 16 min and 24 min for 2000 ppm and 500 ppm toluene respectively. Compared with our previous study, P3HT/PCBM sensing chip showed longer response time (~120 min) for 500 ppm toluene detection [25]. The P3HT/PMMA fibrous film could effectively detect the lower explosive limit (LEL) that is the minimum concentration of a VOC vapor necessary to support its combustion in air. The LEL of ethanol, acetone, toluene, *o*-xylene and chlorobenzene are 33,000, 26,000, 12,000, 10,000 and 18,000 ppm, respectively (Table 2) [25,39]. The developed P3HT/PMMA fibrous film in this study can achieve the basis of the instant response to the concentration of explosive limit. We also measured the reversibility of P3HT/PMMA fibrous film as shown in Fig. 9. For 10,000 ppm toluene exposure, the maximum response declined from 0.81% to 0.67% after three cycles of response testing. For low concentration toluene exposure, the maximum response declined from 0.38% to 0.33% for 2000 ppm toluene exposure and no decay for 500 ppm toluene exposure after three cycles of response testing. The results indicate that P3HT/PMMA fibrous film is degraded due to the fibrous film exposed to the high concentration of toluene. For 10,000 ppm of toluene exposure, the response was returned to the original point after 42 min. For 2000 and 500 ppm of toluene exposure, the response was returned to the original point after 29 min and 18 min, respectively. For the low concentration toluene testing, the adsorption/desorption cycles of toluene showed the acceptable reversibility. For the differences between the commercialized VOCs sensor and P3HT/PMMA fibrous film, the commercialized sensor analyzes VOCs by photoionization detector (PID). Although PID exhibits the high sensitivity for detecting aromatic compounds, the signals are affected by moisture easily. In contrast, P3HT/PMMA fibrous film is not affected by moisture (Fig. 8(a)). Hence, the low-cost P3HT/PMMA fibrous film developed in the present work extends the current VOCs sensing technology.

4. Conclusion

The VOCs sensing materials consisted of P3HT/PMMA blending were prepared successfully by electrospinning process in this study. A series of VOCs, *e.g.* ethanol, acetone, toluene, *o*-xylene and chlorobenzene were chosen to test the sensitivity of P3HT/PMMA fibrous film. The P3HT/PMMA fibrous film can effectively detect the lower explosive limit for VOCs, and it even can achieve the detection limit of acetone, toluene and *o*-xylene at 500 ppm. This low-cost P3HT/PMMA fibrous film developed in the present work extends the current VOCs sensing technology. It can be extensively used to protect humans and the environment from VOCs potential risks.

Supplementary materials

Supplementary material associated with this article can be found, in the online version, at doi:10.1016/j.jtice.2017.06.036.

References

[1] Rahman MM, Balkhoyor HB, Asiri AM, Sobahi TR. Development of selective chloroform sensor with transition metal oxide nanoparticle/multi-walled carbon nanotube nanocomposites by modified glassy carbon electrode. J Taiwan Inst Chem Eng 2016;66:336–46.

[2] Zarifi MH, Sohrabi A, Shaibani PM, Daneshmand M, Thundat T. Detection of volatile organic compounds using microwave sensors. IEEE Sens J 2015;15:248–54.

[3] Yamagiwa H, Sato S, Fukawa T, Ikehara T, Maeda R, Mihara T, et al. Detection of volatile organic compounds by weight-detectable sensors coated with metal-organic frameworks. Sci Rep 2014;4:6247.

[4] Al-Salman HS, Abdullah MJ. Preparation of ZnO nanostructures by RF-magnetron sputtering on thermally oxidized porous silicon substrate for VOC sensing application. Measurement 2015;59:248–57.

[5] Yu X, Zhou N, Han S, Lin H, Buchholz DB, Yu J, et al. Flexible spray-coated TIPS-pentacene organic thin-film transistors as ammonia gas sensors. J Mater Chem C 2013;1:6532–5.

[6] Hirschmann CB, Koivikko NS, Raittila J, Tenhunen J, Ojala S, Rahkamaa-Tolonen K, et al. FT-IR-cPAS—new photoacoustic measurement technique for analysis of hot gases: a case study on VOCs. Sensors 2011;11:5270.

[7] Hirschmann CB, Sinisalo S, Uotila J, Ojala S, Keiski RL. Trace gas detection of benzene, toluene, p-, m- and o-xylene with a compact measurement system using cantilever enhanced photoacoustic spectroscopy and optical parametric oscillator. Vib Spectrosc 2013;68:170–6.

[8] Bai H, Shi G. Gas sensors based on conducting polymers. Sensors 2007;7:267–307.

[9] Savage N, Chwieroth B, Ginwalla A, Patton BR, Akbar SA, Dutta PK. Composite n–p semiconducting titanium oxides as gas sensors. Sens Actuator B 2001;79:17–27.

[10] Lonergan MC, Severin EJ, Doleman BJ, Beaber SA, Grubbs RH, Lewis NS. Array-based vapor sensing using chemically sensitive, carbon black–polymer resistors. Chem Mat 1996;8:2298–312.

[11] Kilinc N, Cakmak O, Kosemen A, Ermek E, Ozturk S, Yerli Y, et al. Fabrication of 1D ZnO nanostructures on MEMS cantilever for VOC sensor application. Sens Actuator B 2014;202:357–64.

[12] Wang Y, Yeow JTW. A review of carbon nanotubes-based gas sensors. J Sens 2009;2009:493904.

[13] Shin J, Choi S-J, Youn D-Y, Kim I-D. Exhaled VOCs sensing properties of WO3 nanofibers functionalized by Pt and IrO2 nanoparticles for diagnosis of diabetes and halitosis. J Electroceram 2012;29:106–16.

[14] Faisal M, Khan SB, Rahman MM, Jamal A, Abdullah MM. Fabrication of ZnO nanoparticles based sensitive methanol sensor and efficient photocatalyst. Appl Surf Sci 2012;258:7515–22.

[15] Sun B, Li X, Zhao R, Yin M, Wang Z, Jiang Z, et al. Hierarchical aminated PAN/γ–AlOOH electrospun composite nanofibers and their heavy metal ion adsorption performance. J Taiwan Inst Chem Eng 2016;62:219–27.

[16] Li X, Teng K, Shi J, Wang W, Xu Z, Deng H, et al. Electrospun preparation of polylactic acid nanoporous fiber membranes via thermal-nonsolvent induced phase separation. J Taiwan Inst Chem Eng 2016;60:636–42.

[17] Yarin AL, Koombhongse S, Reneker DH. Taylor cone and jetting from liquid droplets in electrospinning of nanofibers. J Appl Phys 2001;90:4836–46.

[18] Doshi J, Reneker DH. Electrospinning process and applications of electrospun fibers. J Electrost 1995;35:151–60.

[19] Ding B, Wang M, Yu J, Sun G. Gas sensors based on electrospun nanofibers. Sensors 2009;9:1609.

[20] Ding B, Wang M, Wang X, Yu J, Sun G. Electrospun nanomaterials for ultrasensitive sensors. Mater Today 2010;13:16–27.

[21] Treat ND, Shuttle CG, Toney MF, Hawker CJ, Chabinyc ML. In situ measurement of power conversion efficiency and molecular ordering during thermal annealing in P3HT:PCBM bulk heterojunction solar cells. J Mater Chem 2011;21:15224–31.

[22] Brady MA, Su GM, Chabinyc ML. Recent progress in the morphology of bulk heterojunction photovoltaics. Soft Matter 2011;7:11065–77.

[23] Wang H, Shah M, Ganesan V, Chabinyc ML, Loo Y-L. Tail state-assisted charge injection and recombination at the electron-collecting interface of P3HT:PCBM bulk-heterojunction polymer solar cells. Adv Energy Mater 2012;2:1447–55.

[24] Irwin MD, Liu J, Leever BJ, Servaites JD, Hersam MC, Durstock MF, et al. Consequences of anode interfacial layer deletion. HCl-treated ITO in P3HT:PCBM-based bulk-heterojunction organic photovoltaic devices. Langmuir 2010;26:2584–91.

[25] Liao H-C, Hsu C-P, Wu M-C, Lu C-F, Su W-F. Conjugated polymer/nanoparticles nanocomposites for high efficient and real-time volatile organic compounds sensors. Anal Chem 2013;85:9305–11.

[26] Matsumoto H, Tanioka A. Functionality in electrospun nanofibrous membranes based on fiber's size, surface area, and molecular orientation. Membranes 2011;1:249–64.

[27] Khan M, Chen M, Wei C, Tao J, Huang N, Qi Z, et al. Synthesis at the nanoscale of ZnO into poly(methyl methacrylate) and its characterization. Appl Phys A 2014;117:1085–93.

[28] Chun YT, Neeves M, Smithwick Q, Placido F, Chu D. High optical and switching performance electrochromic devices based on a zinc oxide nanowire with poly(methyl methacrylate) gel electrolytes. Appl Phys Lett 2014;105:193301.

[29] Kuo C-C, Wang C-T, Chen W-C. Poly(3-hexylthiophene)/poly(methyl methacrylate) core-shell electrospun fibers for sensory applications. Macromol Symp 2009;279:41–7.

[30] Chen J-Y, Wu H-C, Chiu Y-C, Lin C-J, Tung S-H, Chen W-C. Electrospun poly(3-hexylthiophene) nanofibers with highly extended and oriented chains through secondary electric field for high-performance field-effect transistors. Adv Electron Mater 2015;1:1400028.

[31] Loewe RS, Khersonsky SM, McCullough RD. A simple method to prepare head--to-tail coupled, regioregular poly(3-alkylthiophenes) using grignard metathesis. Adv Mater 1999;11:250–3.

[32] Wu M-C, Liao H-C, Chou Y, Hsu C-P, Yen W-C, Chuang C-M, et al. Manipulation of nanoscale phase separation and optical properties of P3HT/PMMA polymer blends for photoluminescent electron beam resist. J Phys Chem B 2010;114:10277–84.

[33] Flory PJ. Thermodynamics of high polymer solutions. J Chem Phys 1942;10:51–61.

[34] Huggins ML. Solutions of long chain compounds. J Chem Phys 1941;9:440.

[35] Wu M-C, Chang C-H, Lo H-H, Lin Y-S, Lin Y-Y, Yen W-C, et al. Nanoscale morphology and performance of molecular-weight-dependent poly(3-hexylthiophene)/TiO$_2$ nanorod hybrid solar cells. J Mater Chem 2008;18:4097–102.

[36] Kim Y, Cook S, Tuladhar SM, Choulis SA, Nelson J, Durrant JR, et al. A strong regioregularity effect in self-organizing conjugated polymer films and high-efficiency polythiophene:fullerene solar cells. Nat Mater 2006;5:197–203.

[37] Liao W-P, Wu J-J. Efficient electron collection in hybrid polymer solar cells: in--situ-generated ZnO/poly(3-hexylthiophene) scaffolded by a TiO$_2$ nanorod array. J Phys Chem Lett 2013;4:1983–8.

[38] Zeng T-W, Liu IS, Huang K-T, Liao H-C, Chien C-T, Wong DK-P, et al. Effects of bifunctional linker on the optical properties of ZnO nanocolumn-linker-CdSe quantum dots heterostructure. J Colloid Interface Sci 2011;358:323–8.

[39] https://www.mathesongas.com/pdfs/products/Lower-(LEL)-&-Upper-(UEL)-Explosive-Limits-.pdf